NJOC-CPR(18) 19902

ML Richiusa et al.

# Maximizing JET divertor mechanical performance for the upcoming Deuterium-Tritium experiments

Preprint of Paper to be submitted for publication in Proceeding of
30th Symposium on Fusion Technology (SOFT)

This work has been carried out within the framework of the EUROfusion Consortium and has received funding from the Euratom research and training programme 2014-2018 under grant agreement No 633053. The views and opinions expressed herein do not necessarily reflect those of the European Commission.

# Maximizing JET divertor mechanical performance for the upcoming Deuterium-Tritium experiments

M. L. Richiusa[a], D. Iglesias[a], G. F. Matthews[a], M. Porton[a], V. K. Thompson[a], Z. Vizvary[a].

[a]*UKAEA-CCFE, Culham Science Centre, Abingdon, Oxon, OX14 3DB, UK*

The next D-T campaign will push the JET ITER-like wall to high divertor power and energy levels. During the 2016 campaign, Strike Point (SP) sweeping permitted relevant H-mode scenarios without exceeding the temperature limits imposed by JET Operation Instructions (JOIs). In the subsequent shutdowns, six outer divertor tungsten-coated 2D carbon fibre composite tiles were found to have inter-laminar cracks.

Here we describe the results of a 3D thermo-mechanical analysis aimed at understanding the origin of the cracks. A sensitivity assessment has been carried out on the temperature time-evolution of a realistic tile 3D model during high power pulses, both with fixed and sweeping SPs. Time and space-varying heat flux density loads on the divertor have been calculated using different techniques for reconstructing the power footprint. The results have been benchmarked against the temperature measurements by high resolution infrared diagnostic systems.

The study confirmed the source of the cracks and their localization in the upper part of the tile, giving inter-laminar tension higher than the Ultimate Tensile Stress. Plasma input power, radial location of the SP and sweeping amplitude play an important role on the stress field whose maximum value strongly depends on the SP location. Their influence on the maximum stress value has been investigated and optimized to maximize the performance of divertor tiles without exceeding the limits on input energy and maximum surface temperature imposed by the JOIs.

Keywords: JET, Divertor integrity, ILW, D-T preparation, Synthetic plasma pulses, Experimental validation.

## 1. Introduction

The Joint European Torus (JET) is the world largest tokamak and the only one able to operate with tritium. The upcoming experimental campaign will be of great importance for ITER, foreseeing the exploration of isotope effects on transport, confinement, L-H mode transition, pedestal physics, and plasma-wall interaction by operating with $H_2$, $D_2$ and $T_2$ using the ITER-Like Wall (ILW). Going towards its second D-T campaign (DTE2), JET will be pushed to much higher power levels. Every operational scenario must comply with the JET Operating Instructions (JOIs) [1] that define limits on JET experiments to prevent excessive heat loads on Plasma Facing Components (PFCs). As the JET divertor targets are inertially cooled, these limits are imposed on plasma input energy and on maximum surface temperatures.

The 2015-16 JET experimental campaign, enhancing the High-performance plasma scenario in preparation for the DTE2, was characterized by plasma pulses performed by sweeping the Strike Point (SP) [2]. This technique permitted high power pulses for longer without exceeding the temperature limits on the divertor surface where the hot exhaust plasma streams along the open magnetic field lines, Figure 1. The divertor targets holding the SP are the inboard vertical (3) and horizontal (4) tile rows and the outboard horizontal (6) and vertical (7) tile rows near the pumping duct entrance. After the installation of the JET ILW [3], the divertor tiles are all made of 2D Carbon Fibre Composite (CFC) covered by a thin layer of tungsten (~20μm) except the central row (5) that is made of bulk tungsten.

Although the last campaign was one of the most successful for improving plasma physics understanding, cracks were subsequently found in six Tile 6s. The cracks extended radially along inter-laminar planes. Initially it was not known whether the cracks were superficial (coating delamination damage) or through-thickness of the upper part of the tile (Figure 2). Sometimes the cracks were accompanied by droplets on the upper surface.

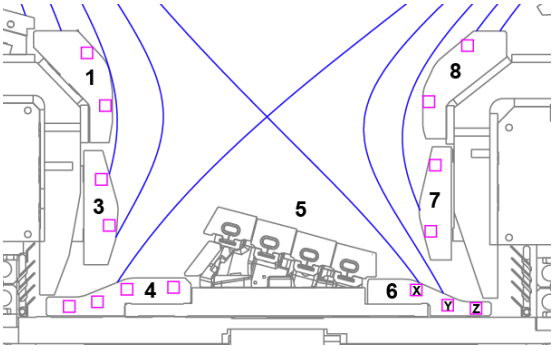


Figure 1. Cross section of the JET divertor after the ILW installation.

Tile 6 integrity is fundamental for DTE2 scenario as it is the most requested target. Risks connected to its failure are: 1. release of particle impurities into the plasma; 2. tritium absorption by CFC; 3. tile erosion on the high-flux side. In addition, previous studies on the failure of the tie rods designed to hold the CFC plies together showed that they don't prevent tile cracking since the tile itself is stiffer than the tie rod [4], and this poses a risk of a combined failure leading to complete tile breakage inside the machine. To reduce the risk of further failure during the upcoming JET restart phase, the cracking damage has led to a deep investigation of the thermo-mechanical behavior of Tile 6. The study, based on modelling the real-time heat load acting on the tile surface, aims to find a relation between the tile stresses and the range of plasma parameters related to this phenomenon.

*Author's email: lorena.richiusa@ukaea.uk*

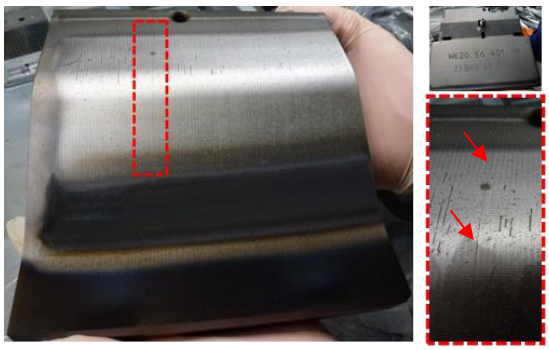

Figure 2. Cracking damage observed on Tile 6.

## 2. Characterization of the failure mechanism

The risk of delamination of tungsten coating due to the thermally-induced carbidisation and consequently embrittlement of the interface requires real-time protection during operations. Infra-Red (IR) thermography based on image diagnostics (IR Cameras) has been installed and upgraded [5] for building the Vessel Thermal Map (VTM), detecting hot spots on PFCs and, if necessary, stopping pulses. In this study, the thermal measurements of scientific IR cameras will be used as a reference for validating the results.

The main issue is the calculation of a realistic heat flux load on the divertor tile. Using Finite Element (FE) modelling for transient thermo-mechanical analyses, the study can be divided into two phases characterized by two different assumptions on computing the realistic heat load on the tile surface:

- Phase 1: capturing of the failure modes using IR-derived heat flux loads calculated through inverse analyses [6] and identification of the main machine parameters affecting the behavior of the tile.
- Phase 2: creation of synthetic shots linked to the next C38 campaign using a convolution of a Gaussian with an exponential profile (Eich's function) for calculating the power footprint on the tile surface [7].

### 2.1 Geometry, FE model and materials

The Tile 6 FE model is shown in Figure 3. Tie rods are not needed in this work according to what explained in §1. The tile is made of CFC plies stacked along the toroidal direction (ϕ-axis in Figure 3), covered by 20 μm tungsten layer. The model includes the temperature dependence and orthotropic nature of the CFC.

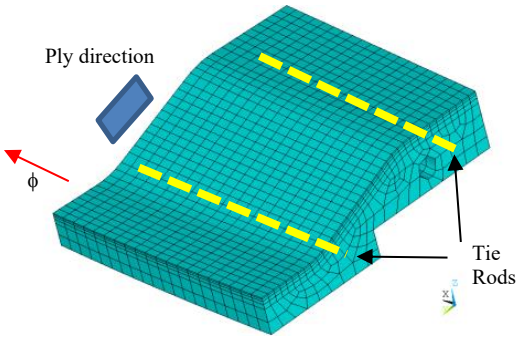


Figure 3. Tile 6 FE model.

From the structural point of view, isostatic constraints have been imposed on Tile 6 FE model.

### 2.2 Phase 1: cracking damage investigation

Table 1 shows the pulses of interest from the last campaign. Two fixed SP pulses (denoted with the subscript 'f') and two swept pulses (denoted with the subscript 's') have been chosen.

Table 1. JET Pulse Numbers (JPN) of interest.

| JPN | Experiment | $I_p$ [MA] | $B_T$ [T] | SP [m] | NBI [MW] | Δt [s] |
|---|---|---|---|---|---|---|
| **89297$_f$** | M15-02 Hybrid scenario for D-T | 1.9 | 1.4 | ~0.24 | 13.0 | 7.0 |
| **90287$_f$** | M15-02 Hybrid scenario for D-T | 1.9 | 1.4 | ~0.24 | 13.4 | 7.5 |
| **90271$_s$** | M15-02 Hybrid scenario for D-T | 2.4 | 2.8 | 0.24-0.27 | 17.0 | 7.5 |
| **92025$_s$** | M15-02 Hybrid scenario for D-T | 2.5 | 2.9 | 0.24-0.27 | 23.5 | 5.5 |

Applying IR-derived heat flux loads on the tile surface and a Toroidal Wetted Fraction (TWF) of 70%, a good agreement (within 15%) between the experimental data and the modelled $T_{MAX}$ time-evolution has been obtained for all the pulses (Table 2). The results obtained in Phase I (in terms of $T_{MAX}$ and $\sigma_{MAX}$ vs time) will be used as a reference for the validations made in Phase II.

Table 2. Summary of experimental and FEM data for each pulse for Tile 6.

| JPN | Thermal Results | | | | Mechanical Results |
|---|---|---|---|---|---|
| | Experimental Data | | FEM Data | | |
| | $T_{MAX}$ [°C] | $E_{th,DIV}$ [MJ] | $T_{MAX}$ [°C] | $E_{th,DIV}$ [MJ] | Toroidal stress [MPa] |
| **89297$_f$** | 873 | 32.02 | 794 | 29.76 | 6.05 |
| **90287$_f$** | 1039 | 36.48 | 848 | 36.48 | 7.61 |
| **90271$_s$** | 1017 | 50.84 | 918 | 48.00 | 7.32 |
| **92025$_s$** | 1107 | 39.82 | 936 | 33.83 | 6.76 |
| **92025$_s$_1.12*** | 1107 | 39.82 | 1194 | 38.40 | 8.05 |

*: same JPN:92025 whose thermal energy input the divertor has been incremented by 12%.

In the following, the results related to JPN:92025 are reported in terms of comparison between $T_{MAX,IR}$ and $T_{MAX,FEM}$ time-evolution trends (Figure 4) with temperature and stress contour plots (Figure 5) related to the time instant in which their maximum values are reached. These results are representative of the results obtained for all the pulses analyzed.

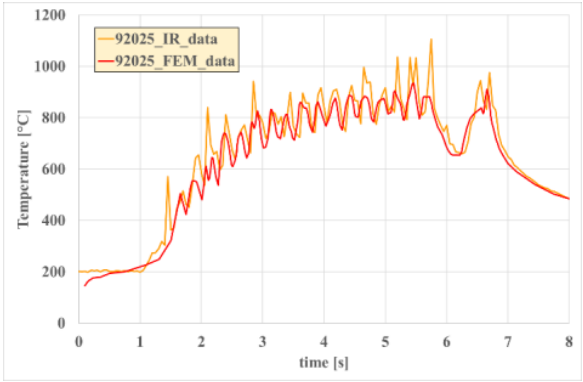


Figure 4. Comparison between experimental $T_{MAX}$ and modelled $T_{MAX}$ – JPN: 92025.

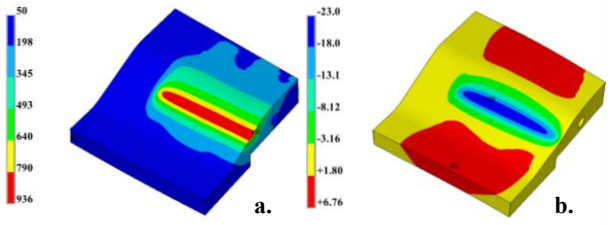


Figure 5. ***(a.)*** Time-instant thermal field [°C] and ***(b.)*** related stress field distribution [MPa] on Tile 6 for JPN: 92025 swept pulse.

### 2.3 Phase 1 preliminary conclusions

The results show the synergic effects of two large thermal gradients: radial and vertical. The radial gradient (~800°C) on the top surface between the central area intersected by the SP and the cooler sides (Figure 5a) leads to central compression and tension on the sides (Figure 5b). These side tensile stresses tend to delaminate the tile and are exactly where the cracks appeared (Figure 2) and of magnitude consistent with local failure (the inter-laminar tensile strength is about 7 MPa). This effect is enhanced by the vertical thermal gradient which causes a toroidal bending of the tile with increased tension on the top surface. The relation between these stresses and the tile thermal energy will be discussed later.

## 3. Phase II: sensitivity analysis using synthetic pulses

The limited number of high-resolution pulses, the good agreement with the IR data obtained in Phase I and the need to investigate the relation between stress field and operational parameters (SP position, sweeping amplitude) led to a sensitivity analysis based on *synthetic* shots. **Synthetic shot**: discharge related to the up-coming JET C38 campaign simulated imposing constant values of NBI, ICRH and Ohmic power for 6-7 seconds and using Eich's function for the heat load profile (engineering power footprint) by imposing engineering and plasma parameters ($B_t$, $I_p$, $n_e$, $f_{ELM}$) [8]. What is important for this study is an estimation of the average bulk effect of all the power loads acting on the tile. The methodology uses three main steps summarized in Table 3.

Table 3. Summary of the methodology steps.

| **Methodology** | | | |
|---|---|---|---|
| Rationale | Stages | Data | Outcome |
| **Validation against existing discharges** | **Step I** | ***Read from JET database:*** ▪ $B_t$, $I_p$, $n_e$, $f_{ELM}$ ▪ NBI, ICRH, Ohmic power | engineering footprint vs IR-derived heat flux (checks in $T_{MAX}$ and $\sigma_{MAX}$) |
| | **Step II** | ***Imposed constant values:*** ▪ $B_t$, $I_p$, $n_e$, $f_{ELM}$ ▪ NBI, ICRH, Ohmic power | synthetic swept pulses against IR-derived data (checks in $T_{MAX}$ and $\sigma_{MAX}$) |
| **Synthetic shots** | **Step III** | ***Imposed constant values:*** ▪ $B_t$, $I_p$, $n_e$, $f_{ELM}$ ▪ NBI, ICRH, Ohmic power | JET C38 experimental campaign synthetic shots and sensitivity analysis |

Step I validates the power footprint against IR-derived heat flux. Step II validates the swept shots of Table 1 recreated synthetically against IR-derived data. Step III is independent of existing experimental data and studies the effect of operational parameters on the tile mechanical stress using synthetic shots.

### 3.1 Step I: engineering footprint vs IR-derived heat flux

The two swept shots of Table 2 have been run using the engineering power footprint [8] for modelling the power density on the tile surface. Compared to the results using IR-derived heat loads (Phase I) taken as reference, the error on $T_{MAX}$ and $\sigma_{MAX}$ is about 13% and 38%, respectively. Overall, the power footprint gives a good estimation of the heat load, but it needs to be refined during the up-coming restart phase. Main limitations: an average value of $n_e$ (1.4E+20 $m^{-2}$) and $f_{ELM}$ (40 Hz) is imposed during the shot.

### 3.2 Step II: synthetic pulses vs IR-derived data

The two swept shots of Table 2 have been recreated synthetically using as heat load the power footprint validated in Step I and imposing from scratch the plasma power input, preserving the experimental thermal energy indicated in Table 2. The power going into the SOL has been estimated according to the following conservative assumptions: 1. NBI and ICRH power input assumed constant for 6-7 seconds; 2. constant radiated power loss by fraction of 30% ($P_{RAD}=0.3 \cdot P_{TOT,plasma}$). The power density on the divertor surface estimated through forward analyses [6] has been applied in the thermo-mechanical FE model giving promising results that will be reviewed during the JET experiments. The error obtained on $T_{MAX}$ and $\sigma_{MAX}$ is of the same order of magnitude as before.

Having validated the procedure against existing pulses, the study has been carried on without relying on existing experimental data.

### 3.3 Step III: synthetic pulses and sensitivity analysis

This step creates new pulses for Hybrid and Baseline scenarios planned for the next JET campaign. Two different power levels have been set, according to the availability of the NBI (30 and 40 MW), as well as different values for SP location and sweeping amplitude. The sensitivity analysis examines how the last two variables affect the thermally-induced stress for a fixed power level. For every SP location (2.85, 2.90, and 2.95 m major radii – $SP_1$, $SP_2$, $SP_3$, respectively, in Figure 6), two different sweeping amplitudes have been considered (0.03-0.06 m, respectively indicated with yellow and red markers in Figure 6).

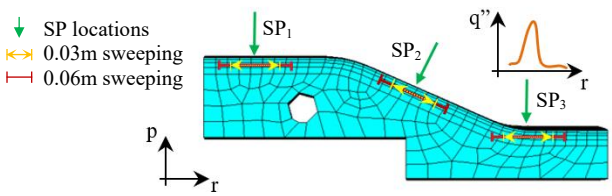


Figure 6. Main parameters involved in the sensitivity analysis.

The sensitivity analysis confirmed the proportionality between Tile 6 toroidal stress and thermal energy input. Figure 7 and Figure 8 show the results, in term of $T_{MAX}$

and $\sigma_{MAX}$ time-evolution, respectively, of the 40 MW pulse with different combinations of SP location and sweeping amplitude. A change in SP location can reduce the stress value by up to 60% when the SP is moved outboard and only slightly affects the $T_{MAX}$. In contrast, change in the sweeping amplitude has beneficial effects in decreasing the $T_{MAX}$.

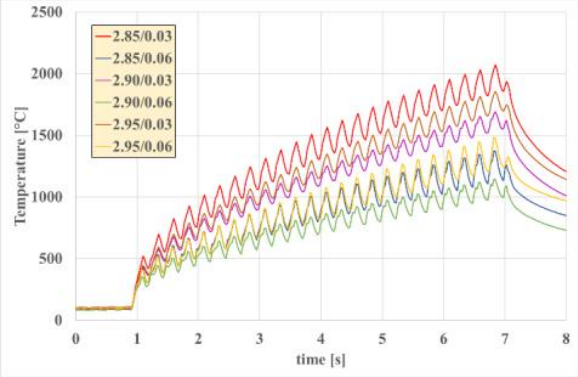


Figure 7. Tile 6 $T_{MAX}$ time-evolution for a 40 MW plasma pulse at different SP locations and sweeping amplitude.

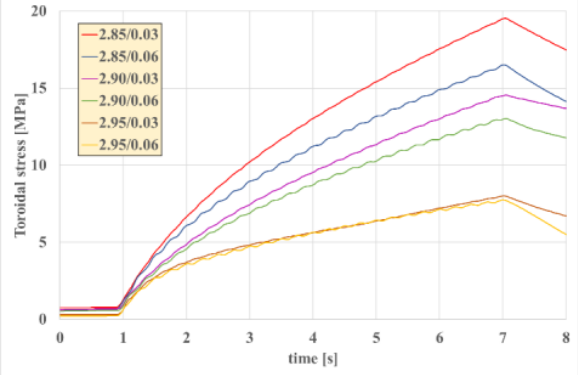


Figure 8. Tile 6 $\sigma_{MAX}$ time-evolution for a 40 MW plasma pulse at different SP locations and sweeping amplitude.

It is worth pointing out that at 4 Hz sweeping frequency, the tiny fluctuations in the stress trend are not a matter of concern for fatigue issue. The stress evolution mainly follows the increase in temperature.

## 3. Conclusions

The cracks found in six JET divertor Tile 6s during the 2017 shutdown have led to an investigation of the thermo-mechanical behavior of Tile 6s under plasma pulses. The study has identified the main operational parameters that can be monitored to avoid further cracking during the upcoming campaign (Figure 6). Preliminary conclusions show the dependency of thermal stress on the energy discharged onto the tile through the SOL, therefore suggesting increasing stress values as the plasma power input increases (red line in Figure 9 representing pulses of Table 2 with different power levels but same SP location).

The sensitivity analysis relevant to the next campaign has underlined that the dominant effect on tile stress is due to the SP position, as Figure 9 clearly shows. Each line indicates three SP positions and the associated pulses with different sweeping amplitude (0.03 and 0.06 m represented using open and closed circle markers, respectively) and different input power levels (30 and 40 MW, indicated with light and dark color for the same sweeping amplitude, respectively). For the most outboard SP at 2.95 m (green line), the sweeping amplitude doesn't have such a significant influence compared with the inboard case (2.85 m). For the 2.95 m case, about 17% of the SOL power is released in Tile 7, so the energy sharing between Tile 6 and Tile 7 can reduce the stress by about 40-60%. The sweeping amplitude has influence on the $T_{MAX}$ but very slight influence on the $\sigma_{MAX}$.

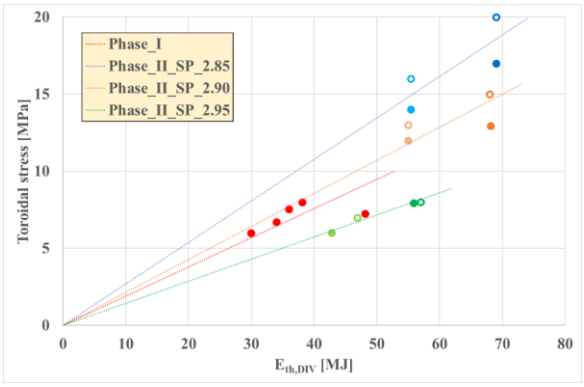


Figure 9. Toroidal stress against Tile 6 thermal energy.

The assumptions and the limitations of the methodology (which will be validated during JET operations) are conservative ($T_{MAX}$ values are higher than expected). This does not affect its goal because it has been useful for understanding the relation among stress, SP location, sweeping amplitude and plasma power levels and in identifying the SP location as the most critical parameter.

Cracks cannot be avoided at energy levels above about 35 MJ, but the tie rods will prevent complete tile failure and allow for remote maintenance. The rods themselves are also vulnerable to failure through fatigue and so their integrity is managed through rationing of high energy pulses.

## Acknowledgments

This work has been carried out within the framework of the Contract for the Operation of the JET Facilities and has received funding from the European Union's Horizon 2020 research and innovation programme. The views and opinions expressed herein do not necessarily reflect those of the European Commission.

## References

[1] D. Stork *et al.,* Fusion Eng. Des. 47 (1999) 131.
[2] S. A. Silburn *et al.,* 2017 *Phys. Scr.* **2017** 014040.
[3] G. F. Matthews *et al.,* 2011 *Phys. Scr.* **2011** 014001.
[4] P. Bunting, *Tile 6 Tie Rod Fatigue Analysis*, IVER_UM_1500_D014, November 2015.
[5] G. Arnoux *et al.,* Review of Scientific Instruments 83, 10D727 (2012); doi: 10.1063/1.4738742.
[6] D. Iglesias *et al.*, *Digital Twin Applications for the JET Divertor*, October 2017.
[7] T. Eich *et al.,* 2013 *Nucl. Fusion* **53** 093031.
[8] V. Riccardo *et al., Power footprint definition for JET divertor protection*, EUROfusion WPJET1-PR (16) 14684.